Dynamics of BaCl- NH Adsorption Pair

Y. Zhong, R.E. Critoph, R.N. Thorpe, Z. Tamainot-Telto

Accepted Manuscript

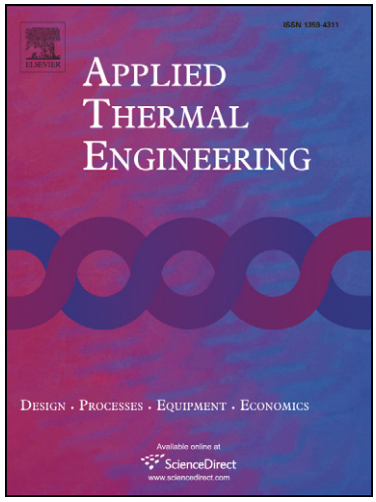

Dynamics of $BaCl_2$ – NH_3 Adsorption Pair

Y. Zhong, R.E. Critoph, R.N. Thorpe, Z. Tamainot-Telto

PII: S1359-4311(08)00271-8
DOI: 10.1016/j.applthermaleng.2008.06.015
Reference: ATE 2541

To appear in: *Applied Thermal Engineering*

Received Date: 12 January 2007
Revised Date: 14 January 2008
Accepted Date: 8 June 2008

Please cite this article as: Y. Zhong, R.E. Critoph, R.N. Thorpe, Z. Tamainot-Telto, Dynamics of $BaCl_2$ – NH_3 Adsorption Pair, *Applied Thermal Engineering* (2008), doi: 10.1016/j.applthermaleng.2008.06.015

Dynamics of $BaCl_2$ – NH_3 Adsorption Pair

Y. Zhong *, R.E. Critoph, R.N. Thorpe, Z. Tamainot-Telto

School of Engineering, University of Warwick, CV4 7AL, UK

Abstract

To obtain accurate kinetics of adsorption pairs, dynamic tests of a composite adsorbent material ($BaCl_2$ impregnated into a vermiculite matrix) and ammonia were performed on small samples under isothermal conditions and on a larger quantity in a laboratory scale adsorption system. The experimental results show that the size of the pressure swing plays an important role in the dynamics of adsorption pairs. This driving pressure difference affects the mass transfer of NH_3 through the pores of adsorbent and therefore the performance of the complete adsorption system. A modified LDF (Linear Driving Force) model was used to fit the experimental results. It was shown that the model can predict the dynamics of both adsorption and desorption fairly well and can be used for the modelling of the adsorption system and adsorption cycles.

Keywords: Dynamics, Sorption rate, Modified LDF model

* Corresponding author. Tel.: +44-2476-523137; Fax: +44-2476-418922
Email address zhongyong77@gmail.com (Yong Zhong)

Introduction

Chemisorption could be useful in adsorption systems due to the large concentration change compared with physisorption. The most commonly used adsorption pairs for chemisorption are metallic salts and ammonia. However, the salt swelling, due to its reaction with ammonia, can damage the matrix structure. It was found that composites of metallic salts impregnated into various porous host matrices can accommodate the swelling and abate the damage. An inorganic salt, expanded vermiculite , is one of the promising host matrices. It allows insertion of a large amount of salt inside the pores, reaching an ammonia uptake of 68.5 wt. % (for a composite "63.5 wt % $BaCl_2$/vermiculite") [1]. And also, it can efficiently accommodate the salt swelling due to its large pore volume.

As we know, for a real adsorption chiller, accurate isotherms, isosteric heat of adsorption and the kinetic characteristics of adsorption and desorption are the key factors to determine the performance of the system [2]. However, most of previous studies on adsorption heat pumps have been performed using steady-state concepts, while a real adsorption system can hardly reach the equilibrium state because of the short cycle time.

Dawoud and Aristov carried out the kinetic study of water sorption on loose grains of composite sorbent $CaCl_2$ confined to meso-porous silica for various grain sizes

(between 0.34 and 3.2 mm) and various salt contents (12.6-33.7 wt.%) [3]. Experimental measurements were performed in a constant pressure unit based on a microbalance under isothermal external conditions [4]. The results showed evidence of a remarkable enhancement of the sorption rate and apparent diffusion constant with the decrease in the particle size and salt content. The kinetic characteristic sorption times were used to evaluate the specific power generated inside adsorbent grains during the water sorption [4]. Aidoun and Ternan performed an experimental study on the effect of the kinetic characteristics of $CoCl_2 - NH_3$ working pairs on the performance of the chemical heat pump [5]. The experimental results showed that the rate of the synthesis reaction in a chemical heat pump is controlled by the rate of diffusion of ammonia gas into the chemical salt [6].

The mathematical models often used to describe the dynamics of adsorption system are LDF (Linear Driving Force) and FD (Fickian Diffusion) model [7 – 11].

The Linear Driving Force (LDF) model for gas adsorption kinetics is frequently and successfully used for analysis of adsorption column dynamic data and for adsorptive process designs because it is very simple. This model was first introduced by Gluekauf [7, 8]. According to the LDF model, the rate of adsorption of adsorbate into adsorbent particles is given by [9]:

$$\frac{d\bar{x}(t)}{dt} = K_L\left(x^* - \bar{x}(t)\right) \tag{1}$$

where, $\bar{x}(t)$ is the average adsorbate concentration in the adsorbent particle at time *t*,

x^* is the final equilibrium adsorbate concentration in the adsorbent particle, K_L is called the effective LDF mass transfer coefficient and usually given by [7],

$$K_L = \frac{15 D_0}{r_0^2} \tag{2}$$

where D_0 is intra-particle diffusivity of sorbate and r_0 is radius of particle or crystal

Another well known model to describe the kinetics of adsorption system is the isothermal Fickian diffusion (FD) model [9]. Compared to the LDF model, the FD model imposes formidable mathematical complication in adsorptive process design because the differential equations of the FD model have to be integrated at the adsorbent particle level. Also, the above integration process must be repeated over many cycles of operation in order to establish the final cyclic-steady-state separation performance of the overall process. As a result, the FD model will generally require large computational times for process simulation under realistic conditions.

On the other hand, the LDF model is much simpler and most importantly it eliminates the integration step at the particle level so it can significantly reduce the computational times required for realistic process simulations. This model with a lumped mass transfer coefficient is very frequently used for practical analysis of dynamic data and for adsorptive process design because it is simple, analytical, and physically consistent [9]. The LDF model may not fit the experimental data very well because its assumptions are not valid in some conditions in which heat transfer and chemcial reaction have great effect on the sorption process. It is also worth pointing

out that in LDF and FD model, the chemical reaction of adsorbate and adsorbent are not considered. Some mathematical models regarding the dynamics of chemical reactions have been proposed recently. But these models are very complicated and the characteristic coefficients in these models are determined by the adsorption pairs used [12 – 14]. In this paper, in order to simplify the dynamic model, the LDF model is modify by considering the chemical kinetics to predict the dynamics.

This paper presents experimental study on dynamics of one composite material (58.7 wt.% $BaCl_2$ impregnated inside vermiculite matrix) for a small sample under isothermal condition and for a larger sample in a laboratory scale adsorption system. For isothermal condition, with the small sample, the reactor was weighed continuously using a magnetic suspension balance. The object was to obtain an instantaneous direct measurement of the salt conversion from the weight measurement. A modified LDF model was proposed to analyze the dynamics of the system. For the labortary scale adsorption system, the temperatures and pressure of the system were measured, and the modified LDF model was applied to describe the dynamics of the adsorption and desorption process. A one dimension mathematical model was used to calculate adsorbent temperature and the concentration change during experiments. The calculated results were compared with the experimental values to verify the accuracy of the modified LDF model.

Experimental and Results

Dynamic tests under isothermal condition

The simplest experimental method to determine the kinetics of sorption systems involves the measurement of sorption curves, under isothermal conditions for a small sample of the adsorbent subjected to a step change in the sorbate pressure. The experimental apparatus consists of Rubotherm ISOSORP 2000 magnetic suspension balance system, glycol water bath system (50 wt.% glycol to make sure that the system can be cooled down to -30^{o}C) and oil bath system，shown in Figure 1. In the system, four thermocouples within the chamber were used to measure the adsorbate temperature and the wall temperature. The system pressure was measured directly with a calibrated Druck PDCR 920 transducer. The resolution of the pressure transducer was 0.35bar/mV and the accuracy is ±1.5%. The mass of the sample was measured by Rubotherm balance system . The adsorbate concentration was calculated by the mass change of the sample during the experiment. The resolution of the equipment was 0.01 mg and the standard deviation of successive measurement was less than ±0.03 mg. The aluminium sample holder (Figure 2) acted as a thermal ballast and its design ensured good thermal contact with the material under test. The mass of the sample and sample holder were 0.2 and 11.2 g respectively. To make sure that the adsorption system was under isothermal condition, the test cell was contained within a jacket, through which heated oil was circulated in order to maintain the temperatures of the vessel and sample constant. Thus the dynamics of the adsorption

was mainly controlled by mass transfer rather than heat transfer.

The sample was prepared by being held at 180°C for at least 10 hours at atmospheric pressure and then kept for 2 hours under vacuum to make sure that all water vapor was eliminated from the sample. The measuring cell was then connected to an evaporator maintained at a temperature between -20 and 50°C until the system reached an equilibrium state. At the beginning of the dynamic tests, the valve separating the reactor and the reservoir was closed and the saturated temperature of the reservoir was changed to a new value. After the adsorbent material and the refrigerant in the reactor had attained thermal and chemical equilibrium, the valve between the reactor and reservoir was opened. The pressure changed to the pressure of the reservoir, causing a rapid rate of concentration change, because the adsorbent bed was at conditions far from equilibrium. The values of temperature, pressure and mass change during this process were recorded. After the kinetic curve had been recorded, the evaporator was disconnected from the measuring cell and its temperature was increased to fix the proper pressure for the next kinetic test.

Typical kinetic curves of ammonia sorption were shown in Figure 3. In Figure 3(a), the test sample was at the temperature of 37°C and the pressure of the system dropped from 5bar down to 2.15bar. It can be seen from Figure 3 that the concentration change of the adsorbent was around 38% during a over a period of of 20 minutes. No more ammonia was desorbed from the sample and the concentration remained at 2.5%,

which is considered as the contribution of vermiculite to the ammonia concentration. Figure 3(b) showed the kinetic curve when the pressure of system dropped from 4.7 down to 4.5 bar at the same temperature. It took around 400 minutes to complete the decomposition, which was around 20 times longer than that of large pressure difference.

The results of the kinetic experiments on $BaCl_2$ – NH_3 showed that the size of the pressure swing played an important role in the dynamics of adsorption pairs. This driving pressure difference affected the mass transfer of NH_3 through the pores of adsorbent and therefore the performance of the complete adsorption system.

For chemisorption, the chemical reaction rate of adsorption pairs is as important as the diffusion of refrigerant into the adsorbent pores. To better match the experimental data, the LDF model was modified to predict the dynamics of $BaCl_2$ and NH_3 adsorption pair, which was given by [15 - 17],

$$\frac{dx}{dt} = \frac{-1}{\frac{C}{\Delta p} + \frac{1}{K\left(x - x_{eq}\right)}} \tag{3}$$

where C is a resistant coefficient due to chemical reaction between the adsorbate and adsorbent, in Pa s and, K is the mass transfer diffusion coefficient in s^{-1}.

In extreme cases for the two terms in the denominator of the right hand side of equation (3), the reaction rate reduces either to the LDF or to a linear function

proportional to the difference between the system pressure and the equilibrium pressure corresponding to the synthesis or decomposition. This latter term might well be vigorously related chemical driving potential but its justification for use here is chiefly empirical.

C and *K* can be obtained by fitting the experimental data: for adsorption *C*=50 Pa s, *K*=-2500 s^{-1}; for desorption, *C*=30 Pa s,*K*=500 s^{-1}. It is worth pointing out that the value of *C* and *K* came from the data fitting of the experimental data.and that the form of equation 3 is chosen as being empirically useful, without necessarily having established it as a true model of all the physical processes involved.

x_{eq} is the final equilibrium adsorbed phase concentration, $\Delta p = p_{transition} - p$, p is the system pressure, $p_{transition}$ is the onset pressure of the synthesis and decomposition transitions and given by [15 - 18],

$$\ln p_{transition} = 4.98\frac{-1000}{T} + 22.26 \qquad (4)$$

where, T is the temperature of reaction bed. The root mean square error (corresponding to the Standard Estimated Error – SEE) is shown in Table 1 ($\Delta p = p_{transition} - p$) . and It is defined as follow:

$$\text{SEE}=\sqrt{\frac{1}{n}\sum_{i=1}^{n}(x_i - x_{cal})^2} \qquad (5)$$

where n is number of experimental data, x is measured concentration, x_{cal} is the calculated concentration through the modified LDF model. The comparison of the typical experimental data and mathematical model is shown in Figure 4 and Figure 5.

From Figure 4 and Figure 5 , we can conclude that the mathematical model described

in equation (3) can used to predict the dynamics of $BaCl_2$ and NH_3 under isothermal conditions. However, during the experiments, the reactor was kept isothermal, which is not consistent with real adsorption systems. The accuracy of this model is still worth testing in conditions where both pressure and temperature change.

Dynamic test in a laboratory scale adsorption system

The experimental rig (as described in Figure 6) consists of a reactor connected with a receiver and three water thermal baths, which were maintained at around 20°C (receiver water bath), 100°C (desorption water bath) and 20°C (adsorption water bath). Four *K*-type thermocouples (two on the generator, which were placed in the centre and on the tube outer wall respectively; another one was placed on receiver outer wall, the other one was placed in the hot water bath) and a pressure transducer which was used to monitor the pressure within the generator were linked to a PC via an interface (Data Shuttle DA-16-TC-AO). A program written with Workbench 2.3 was used to monitor and record the temperatures and the pressure.

In order to measure the amount of liquid collected during the dynamic test, a glass tubing receiver rated to 40 bar at 20°C (20mm OD and 12mm ID) was connected to the generator. The schematic diagram of the receiver is shown in Figure 7. The mass of ammonia collected in the receiver can be calculated by the following expression:

$$m = 36\pi\rho_{NH_3}10^{-6}\Delta h \qquad (6)$$

Where, m is the mass of ammonia collected in the receiver (g); ρ_{NH_3} is the density of

ammonia liquid, Δh is the height of ammonia liquid level (mm).

Initially, the test generator was at ambient temperature (typically 20°C). After typically 16 hours, the system reached equilibrium state. Then the reactor was submerged suddenly into the boiling water bath (at about 100°C). The pressure and temperatures were recorded for the desorption procedure. After around 1 hour almost all of the ammonia in the reactor was desorbed and condensed in the receiver. The reactor was moved suddenly from the hot water bath to the cold water bath (at around 20°C) and the adsorption dynamic test was started. During the dynamic tests, the receiver was kept at around 20°C, controlled by the cold water bath.

A one-dimensional transient heat conduction generator model was used to simulate the dynamics of the set-up. The thermal conductivity of the bed and the contact heat transfer coefficient between the bed and the tube wall were set to be 0.2 W m^{-1} K^{-1} and 150 W m^{-2} K^{-1} [16, 19]. The explicit scheme of finite difference was used in the modelling. To simplify the simulation, the pressure in a single control volume was assumed to be uniform. Therefore, the bed pressure was uniform and the resistance of mass diffusion through the sample pore in the reactor was neglected. The equations used to monitor the transient sorption characteristics were heat and mass conservation and the sorption dynamic equation.

The transient heat and mass transfer is given by the following equation [16, 19]:

$$\left[\rho_s\left(C_{ps}+C_{pa}x\right)+\rho_g C_{pg}\right]\frac{\partial T}{\partial t}=\frac{k_s}{r}\frac{\partial}{\partial r}\left(r\frac{\partial T}{\partial r}\right)-H\frac{\partial x}{\partial t} \tag{7}$$

where:

ρ_s is the sample density, kg/m^3

C_{ps} is the specific heat of the sample, J/(kg K)

C_{pa} is the specific heat of adsorbed ammonia, J/(kg K)

T is the sample temperature, K

t is the time, s

ρ_g is the density of free gaseous ammonia,(kg)

k_s is the thermal conductivity of the sample, W/(m K)

A is the area of conduction for sample = $2\pi(r + \Delta r/2)\,\Delta z$, m^2

H is the heat of sorption which can obtained form the slope of isotherms [16, 17], J/kg

x is the ammonia concentration, kg NH_3/ kg sample

The mass of adsorbed ammonia m_a is a function of the ammonia concentration and is given by:

$$\frac{m_a}{x} = M_s \tag{8}$$

where: M_s is the total mass of the sample, kg

Then, $$\frac{dm_a}{dt} = M_s \frac{dx}{dt} \tag{9}$$

Equation (9) is used to describe the concentration change of adsorption pair.

During the experiments, the system is closed and the total mass of ammonia m_t remains constant and is the sum of the mass of liquid ammonia in receiver, m_r, the free mass of ammonia gas, m_g, and the adsorbed ammonia in the sample porosity, m_a:

$$m_t = m_a + m_r + m_g \tag{10}$$

The ammonia gas is assumed as perfect gas so that the free mass of ammonia gas can be calculated from the ideal gas law by,

$$m_g = \frac{pv}{RT} \tag{11}$$

where, p is the pressure of the system, Pa; v is the void volume of the system, m^3; R is the gas constant, J/(K kg); T is the temperature of the ammonia gas.

The mass of liquid ammonia in receiver, m_r can be calculated by equation (6). Therefore, the rate of change in adsorbed ammonia in the sample porosity can be presented as:

$$m_a = m_t - m_r - m_g \tag{12}$$

The calculated mass of adsorbent ammonia is compared with the simulated results.

The simulation uses the measured tube wall temperature (boundary condition) and ammonia pressure as input. The heat transfer within the bed is based on the conduction through the bed and with the mass transfer. The initial temperature of the generator is assumed uniform. The simulated centre temperature of the reactor and the concentration of the sample are compared with the experimental results.

Figure 8 and 9 showed the comparison of the experimental data and simulation. For adsorption, except the first one or two minutes, the model can predict the centre temperature and the concentration fairly well. The maximum error is around $\pm 10\%$. For the desorption dynamic test, the mathematical model can predict the centre temperature well, while the model underestimated the concentration especially after

30 minutes. The probable reason is that the ammonia gas might have condensed in the horizontal connecting tube or other void volume. Therefore the measured ammonia level in the receiver would be lower than that expected. In other words, the calculated concentration of the sample from experimental data will be greater than ideal situation.

Conclusion

The kinetics of ammonia sorption under isothermal conditions and in a laboratory scale system was studied at T = 20 to 100°C and p = 0.2 to 20 bar. The pressure difference between the reactor and condenser plays an important role in the dynamics of adsorption pairs. The pressure difference affects the mass transfer of NH_3 through the pores of adsorbent and therefore the performance of the complete adsorption system.

A modified LDF model is used to predict the dynamics of the adsorption system using $BaCl_2$ – NH_3. Through the comparison of the experimental data and simulation, the model has been shown to predict the dynamics of both adsorption and desorption fairly well and so can be used for the modelling of adsorption system and adsorption cycles.

References:

[1] V.E. Sharonov, J.V. Veselovskaya, Yu.I. Aristov, Ammonia sorption on composites "$CaCl_2$ in inorganic host matrix": isosteric chart and its performance, Int. J. Low Carbon Thecn., vol.1(3), pp. 191-200, 2006

[2] C.H. Liaw, J.S.P. Wang, R.H. Greenkorn, and K.C. Chao, Kinetics of fixed bed adsorption: a new solution, AIChE Journal, vol.25, p.376, 1979

[3] B. Dawoud, Yu.I. Aristov, Experimental study on the kinetics of water vapor sorption on selective water sorbents, silica gel and alumina under typical operating conditions of sorption heat pumps, International Journal of Heat and Mass Transfer, vol.46, pp.273–281, 2003

[4] Yu.I. Aristov, I.S. Glaznev, A. Freni , G. Restuccia, Kinetics ofwater sorption on SWS-1L (calcium chloride confined to mesoporous silica gel): Influence of grain size and temperature, Chemical Engineering Science, vol.61, pp.1453 – 1458, 2006

[5] Z. Aidoun, M. Ternan, The synthesis reaction in a chemical heat pump reactor filled with chloride salt impregnated carbon fibres: the NH_3–$CoCl_2$ system, Applied Thermal Engineering, vol.22, pp.1943–1954, 2002

[6] Z. Aidoun, M. Ternan, The unsteady state overall heat transfer coefficient in a chemical heat pump reactor: the NH_3–$CoCl_2$ system, Chemical Engineering Science, vol.59, pp.4023 – 4031, 2004

[7] E. Gluekauf, Theory of chromatography, Part 10, Formula for diffusion into

spheres and their application to chromatography, Transactions of the Faraday Society, vol.51, pp. 1540 – 1551, 1955

[8] J.Kaerger, D.M.Ruthven, Diffusion in zeolites and other microporous solids, J.Willy, N.Y., 1992.

[9] S. Sircar, J.R. Hufton, Why does the linear driving force model for adsorption kinetics work?, Adsorption, vol.6, pp.137–147, 2000

[10] J. Karger, D.M. Ruthven, Diffusion in zeolites and other microporous solids, John Wiley & Sons, INC., USA, 1991

[11] Chi Tien, Adsorption calculations and modeling, Butterworth-Heinemann, London, 1994

[12] V. Goetz V, A. Marty, A model for reversible solid-gas reactions submitted to temperature and pressure constraints: simulation of the rate of reaction in solid-gas reactor used as chemical heat pump, Chemical Engineering Science, 47(17-18):4445-4454, 1992

[13] M. Lebrun, B. Spinner, Models of heat and mass transfers in solid-gas reactors used as chemical heat pumps. Chemical Engineering Science, 45(7):1743-1753, 1990

[14] H.B. Lu, N. Mazet, B. Spinner, Modeling of gas-solid reaction – coupling of heat and mass transfer with chemical reaction, Chemical Engineering Science, 51(15): 3829 – 3845, 1996

[15] V.E. Sharonov, J.V. Veselovskaya, Yu.I. Aristov, Y. Zhong, R.E. Critoph, New composite adsorbent of ammonia "$BaCl_2$ in vermiculate" for adsorptive

cooling, CHP (2006), Proc. HPC06, Newcastle, 2006

[16] Y. Zhong, Studies on equilibrium and dynamic characteristics of new adsorption pairs, Ph.D. Dissertation, University of Warwick, 2006

[17] R.E. Critoph, Y. Zhong, S.J. Metcalf, Dynamic modelling of solar thermal cooling using the $BaCl_2$ – ammonia pair, proc. World Renewable Energy Congress, Florence, August 2006

[18] Y. Zhong, R.E. Critoph, R.N. Thorpe, Z. Tamainot-Telto, Yu.I. Aristov, Isothermal sorption characteristics of the $BaCl_2$ – NH_3 pair in a vermiculite host matrix, Applied Thermal Engineering, ATE-2206-628R1, Accepted, 2007

[19] Z. Tamainot-Telto, R.E. Critoph, Cost effective carbon-ammonia generators, Report No ENK5-CT2002-00632-UW1, October 2003, School of Engineering, University of Warwick

Nomenclature

A	Area of conduction for sample, m^2
C	Resistant coefficient due to chemical reaction, Pa s
C_p	Specific heat, J kg^{-1} K^{-1}
D	Intra-particle diffusivity, m^2s^{-1} H Heat of sorption, J kg^{-1}
Δh	Height of ammonia liquid level, m
K	Effective LDF mass transfer coefficient, s^{-1}
	Mass transfer diffusion coefficient, s^{-1}
k	Thermal conductivity , W m^{-1} K^{-1}
m	Mass, kg
p	Pressure, Pa
R	Gas constant, J kg^{-1} K^{-1}
r	*Radius or* Position of the sample cell from the centre, m
Δr	Increment in radius, m
T	Temperature, K
t	Time, s
v	Volume, m^3
x	Mass concentration. kg ammonia kg^{-1} adsorbent
Δz	Total height, m

Subscripts

a	ammonia
eq	equilibrium
g	gas
NH_3	ammonia liquid
r	receiver
s	solid
transition	Synthesis or Decomposition reaction

Greek letter

ρ	Density, kg/m^3
θ	Angle, rad
$\Delta\theta$	Increment in angle, rad

Figure captions

Temperature, ℃	Δp , bar	SEE, %
Desorption		
37.7	2.47	0.35
38.2	0.1	1.87
44.8	3.78	0.13
44.6	0.17	0.91
53.4	5.4	0.59
53.7	0.21	1.16
Adsorption		
38.9	-5.88	0.17
37.9	-6.12	0.33
45.5	-6.35	0.29

Table 1. Standard Estimated Error (SEE)

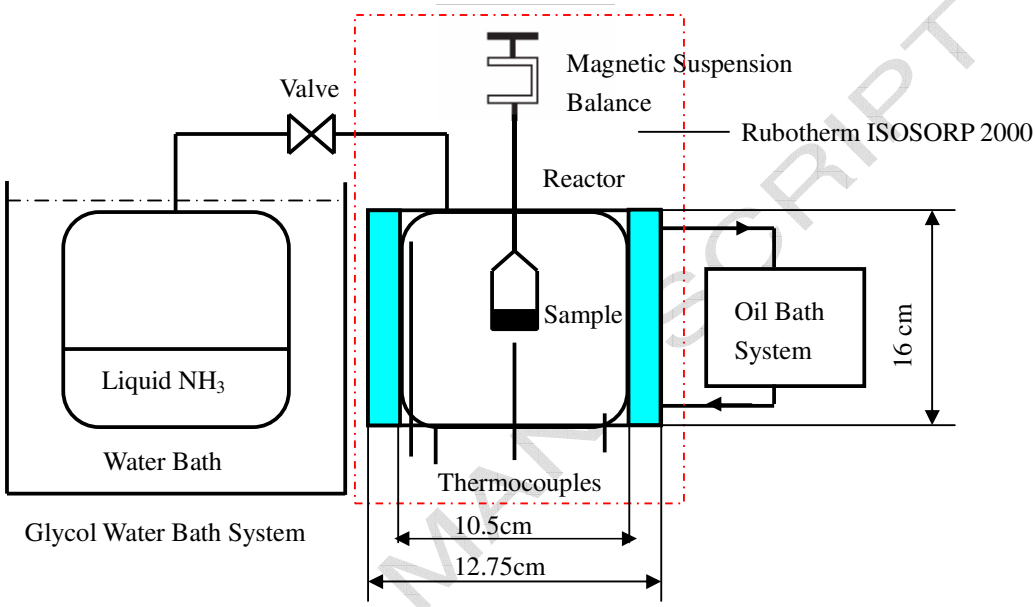

Figure 1 Schematic diagram of porosity test rig

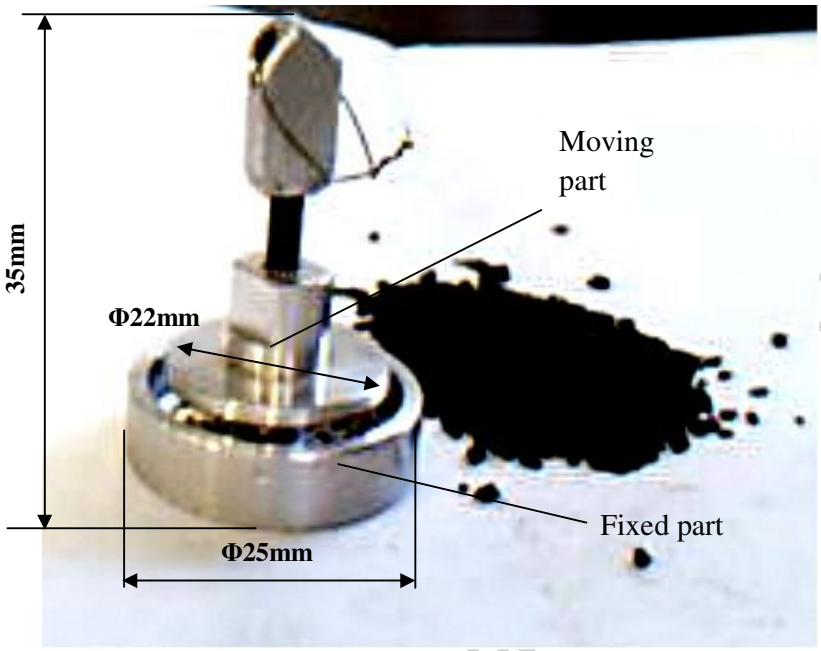

Figure 2 Photograph of the sample holder

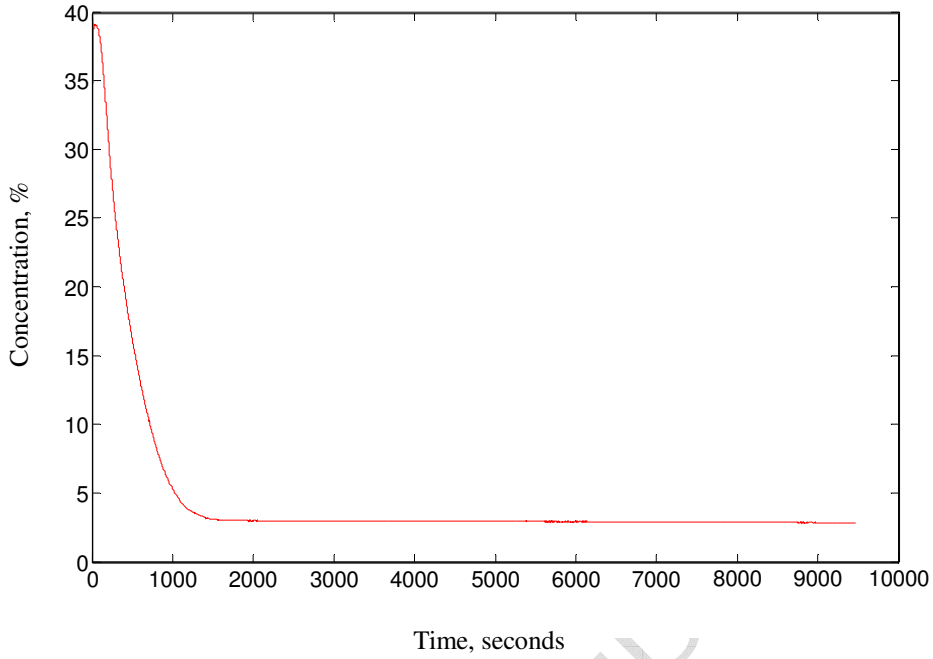

(a) Large pressure difference (pressure drop 2.75bar)

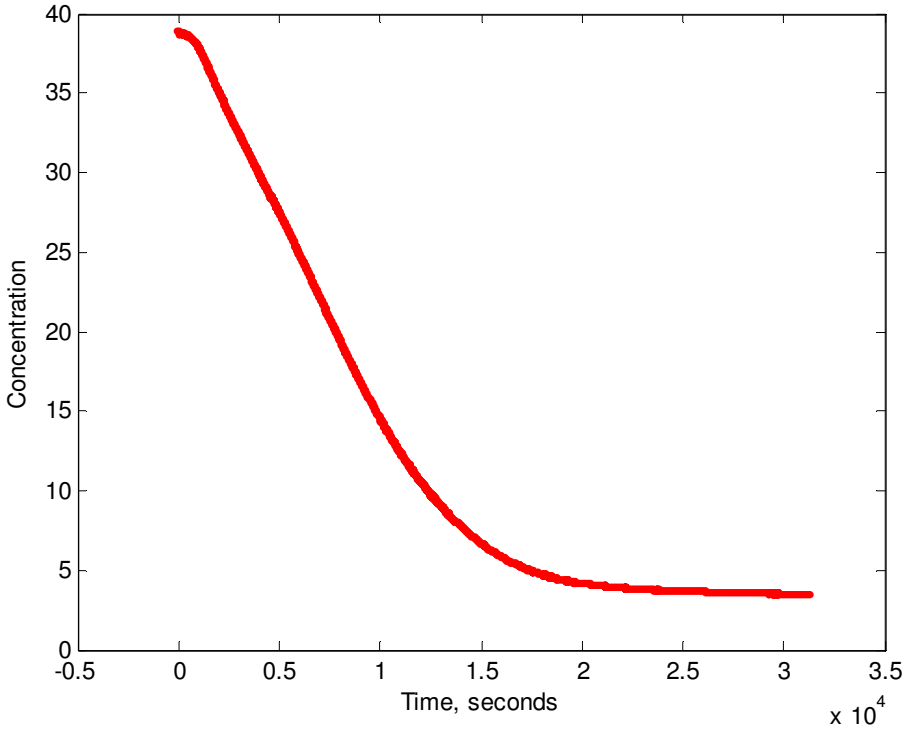

(b) Small pressure difference (pressure drop 0.2bar)

Figure 3 Concentration change against time at 37°C

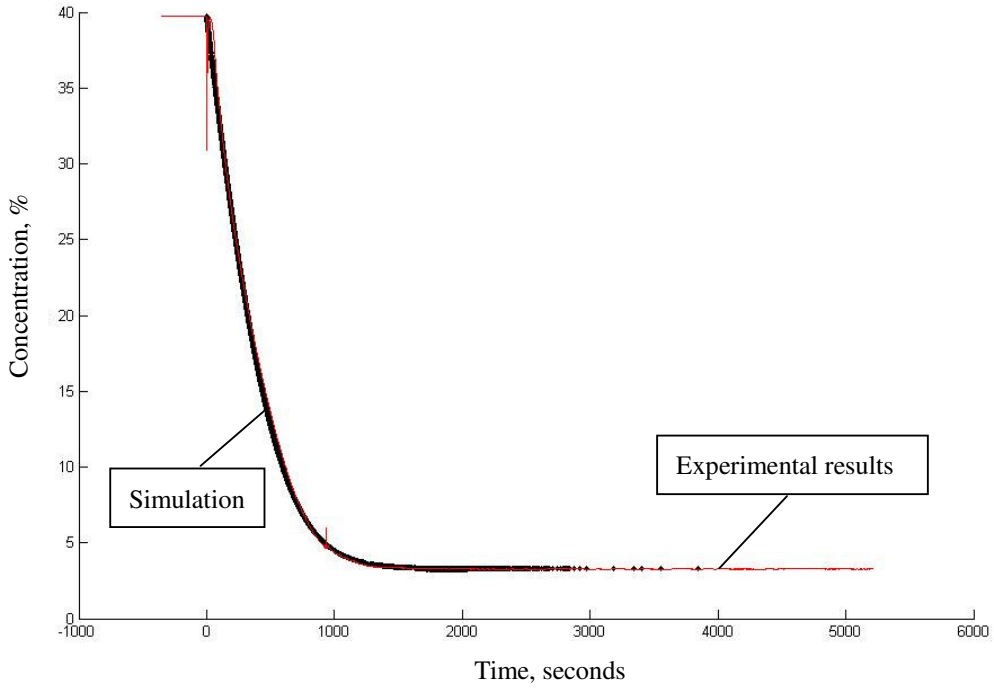

Figure 4 Comparison of desorption experimental data and simulation at T=44.8°C

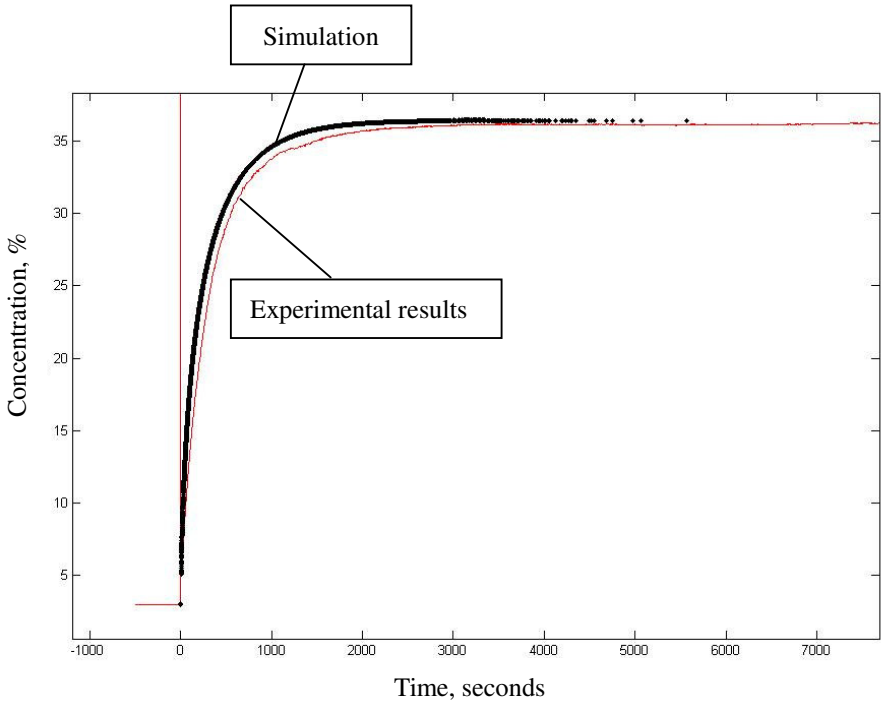

Figure 5 Comparison of adsorption experimental data and simulation at T=45.5°C

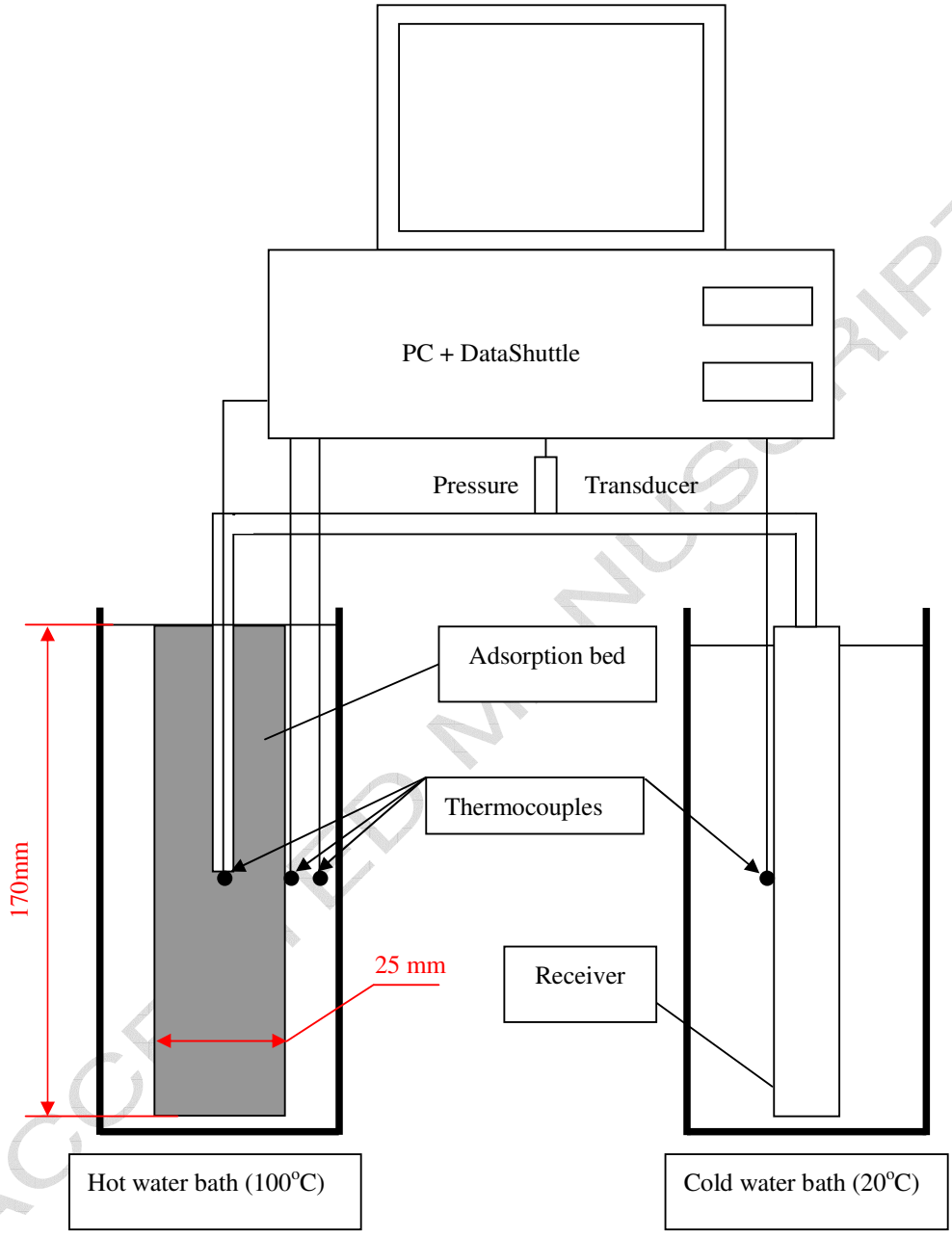

Figure 6 Schematic diagram of the test rig

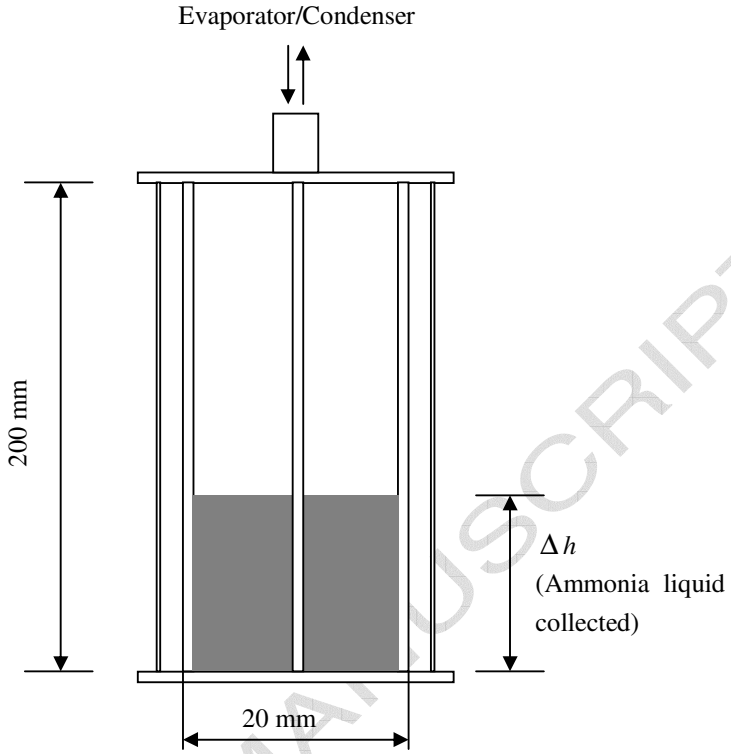

Figure 7 Schematic diagram of the glass tubing ammonia receiver

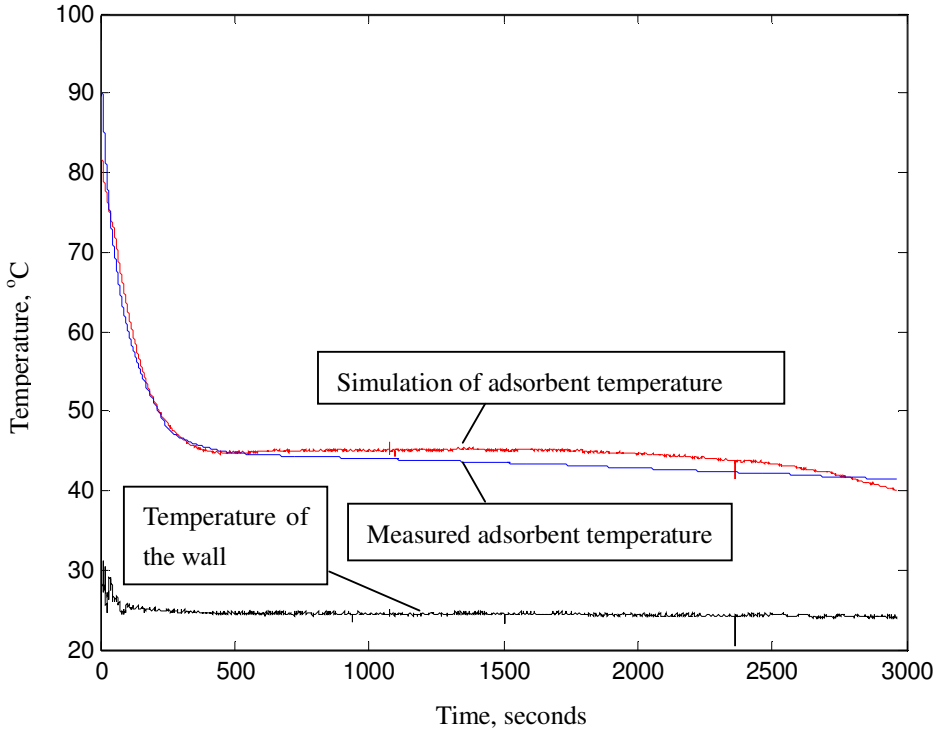

(a) Temperature vs. time

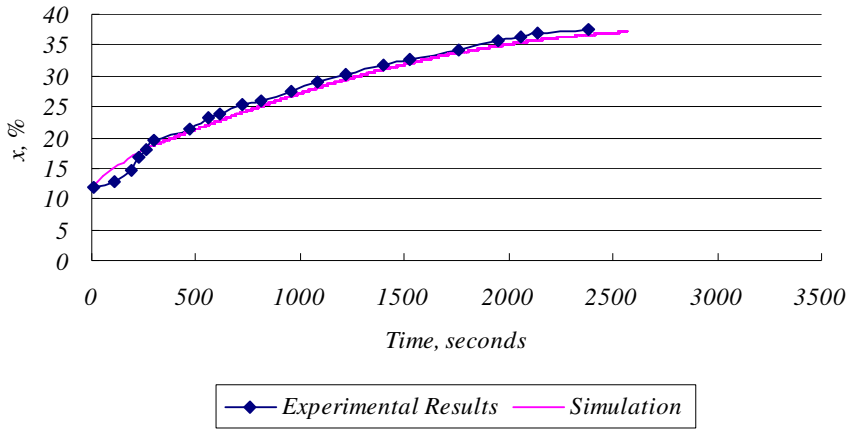

(b) Concentration vs. time

Figure 8 Comparison of adsorption experimental results and mathematical model (the pressure changed from 11.78 to 6.47 bar)

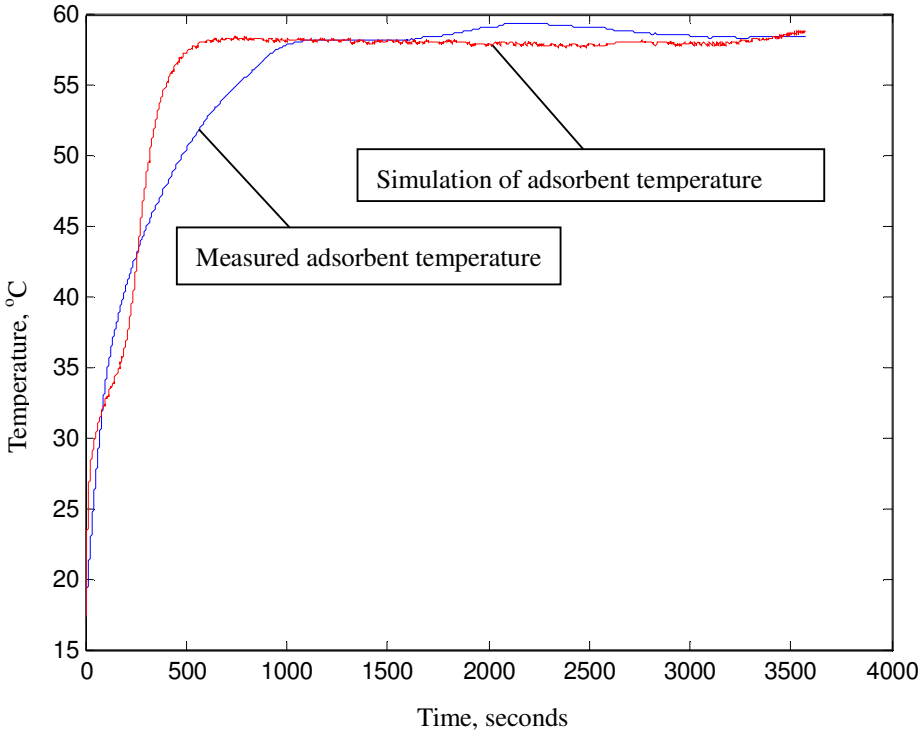

(a) Temperature vs. time

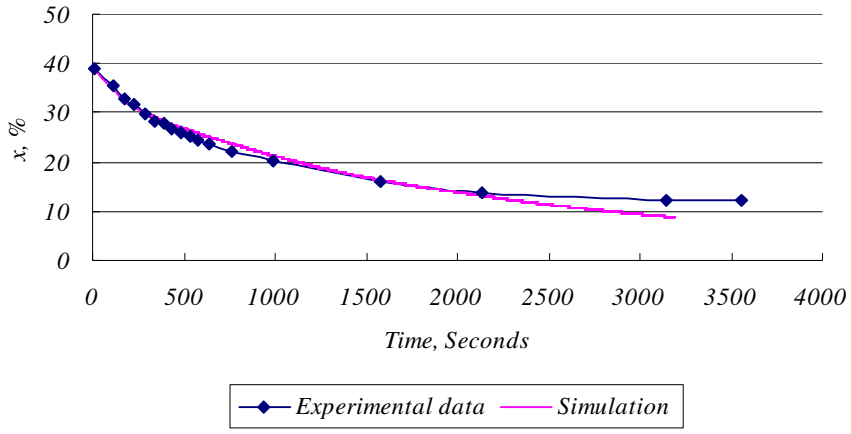

(b) Concentration vs. time

Figure 9 Comparison of desorption experimental results and mathematical model (the pressure changed from 7.99 to 12.78 bar)